

Optical Conductivity of Ferromagnetic Semiconductors

E. H. Hwang⁽¹⁾, A. J. Millis⁽²⁾, S. Das Sarma⁽¹⁾

⁽¹⁾ Condensed Matter Theory Center, Department of Physics, University of Maryland, College Park, MD 20742

⁽²⁾ Department of Physics and Astronomy, Columbia University, 538 W 120th St., New York, NY 10027

The dynamical mean field method is used to calculate the frequency and temperature dependent conductivity of dilute magnetic semiconductors. Characteristic qualitative features are found distinguishing weak, intermediate, and strong carrier-spin coupling and allowing quantitative determination of important parameters defining the underlying ferromagnetic mechanism.

PACS numbers: 75.50.Pp, 75.10.-b, 75.30.Hx, 75.20.Hr

Observations of ferromagnetism in dilute magnetic semiconductors (DMS) [1–4] with transition temperatures as high as 110K (GaMnAs at 5% Mn [1–3]) or even above room temperature (GaMnN, GaMnP [4]) have renewed interest in these remarkable systems [5–11], in part because of possible ‘spintronic’ applications [12]. Several crucial scientific questions have emerged, most notably what parameters control the magnitude of the magnetic transition temperature and how these may be optimized. There is also an urgent need for experimental diagnostics, both for determining fundamental parameters such as the strength of the carrier-spin coupling, and for determining sample-specific parameters such as the carrier density and the degree of spin polarization of the mobile carriers. In this Letter we present theoretical calculations showing that measurements of the optical conductivity $\sigma(\omega, T)$ can be of great help in answering these questions. Optical conductivity measurements have proven useful in understanding the physics of the colossal magnetoresistance (CMR) manganites [13] where carrier-spin coupling is also crucial [14].

We find that the DMS optical conductivity exhibits novel features not found in the CMR. To perform our calculations we use a recently developed non-perturbative method, the ‘dynamical mean field theory’ (DMFT) [15] to calculate $\sigma(\omega, T)$ for the generally accepted model of dilute magnetic semiconductors. A non-perturbative method is needed because the crucial physics involves bound-state formation and other aspects of intermediate carrier-spin couplings not accessible to perturbative methods. The system sizes required for direct numerical simulations for this problem are impractically large, and obtaining accurate dynamical information from numeric is not easy. The DMFT method can handle dynamics easily. Our results display striking, sometimes, counterintuitive, dependence of conductivity on carrier-spin coupling, carrier density, and temperature revealing key features of the underlying physics. Experimental observation of our predictions should lead to crucial information about bound state formation and impurity band physics in this problem.

It is generally believed [11] that DMS are described by the generalized Kondo lattice model

$$H = H_{host} - \sum_{i,\alpha,\beta} J \hat{\mathbf{S}}_i \cdot \psi_\alpha^\dagger(R_i) \vec{\sigma}_{\alpha\beta} \psi_\beta(R_i)$$

$$+ W \psi_\alpha^\dagger(R_i) \psi_\alpha(R_i), \quad (1)$$

where H_{host} describes carrier propagation in the host semiconductor and the second (magnetic) term describes coupling of the carriers to an array of (impurity, e.g. Mn) spins at positions R_i . The coupling has two sources: a spin-spin coupling and a potential scattering. Here we absorb the magnitude of the impurity spin into the coupling J (which we take to be positive), and represent the spin direction by the unit vector $\hat{\mathbf{S}}$. For simplicity we consider a host material with a single non-degenerate band; the extension to the multiband case relevant, for example, to the GaAs valance band is straightforward, involves no new features, and will be presented elsewhere. We therefore write

$$H_{host} = \sum_\alpha \int d^3x \psi_\alpha^+(x) \frac{\nabla^2}{2m} \psi_\alpha(x) + V_R(x) \psi_\alpha^+(x) \psi_\alpha(x), \quad (2)$$

where V_R is a random potential arising from non-magnetic defects in the material.

The crucial physical issues are revealed by the consideration of a ferromagnetic state in which all impurity spins S_i are aligned, say, in the z direction. Then the carriers with spin parallel to S_i feel a potential $-J + W$ on each magnetic impurity site and anti-parallel carriers feel a potential $J + W$. These potentials self-consistently rearrange the electronic structure. The spin-dependent part of this rearrangement provides the energy gain which stabilizes the ferromagnetic state. The key physics issue is, evidently, whether the potential $W \mp J$ is weak (so its effect on carriers near the lower band edge is simply a scattering phase shift) or strong (so only majority spin or perhaps both species of carriers are confined into spin-polarized impurity bands). Recent density functional supercell calculations [16] suggest that in GaMnAs $-J + W$ is close to the critical value for bound state formation for the majority spin systems. Then as temperature is increased, the Mn spins disorder and it is natural to ask how this physics changes. We shall see that all of this behavior is clearly revealed in the optical conductivity, which can therefore be used experimentally to probe the qualitative nature of the magnetic coupling.

To compute the conductivity we write $\nabla \rightarrow (\nabla - ieA/c)$ and apply the usual Kubo formula. To eval-

ate the properties of H we employ the DMFT approximation, which amounts to assuming that the self energy is momentum independent: $\Sigma(p, \omega) \rightarrow \Sigma(\omega)$, so that the Green function $G(p, \omega)$ corresponding to H is $G(p, \omega) = [\omega - p^2/2m - \Sigma(\omega)]^{-1}$. The self energy is given in terms of the solution of an impurity problem [15]. The impurity problem requires a momentum cutoff, arising physically from the electron band-width. We impose the cutoff by assuming a semicircular density of states $D(\epsilon) = \sqrt{4t^2 - \epsilon^2}/2\pi t$ with $t = (2\pi)^{2/3}/mb$ and b^3 the volume per formula unit. The parameter t is chosen to correctly reproduce the band edge density of states. Within this approximation the real part of the conductivity is given by

$$\sigma(\Omega, T) = \int \frac{d^3 p}{(2\pi)^3} \left(\frac{p \cos \theta}{m} \right)^2 \int \frac{d\omega}{\pi} \frac{[f(\omega) - f(\omega + \Omega)]}{\Omega} \times \text{Im}G(p, \omega)\text{Im}G(p, \omega + \Omega), \quad (3)$$

Our approximation for the density of states implies $\int d^3 p/(2\pi)^3 (p \cos \theta/m)^2 \rightarrow \int d\varepsilon D(\varepsilon) \Phi(\varepsilon)$ with $\Phi(\varepsilon) = (4t^2 - \varepsilon^2)/3$ [17].

The main panels of Fig. 1 show the evolution of the conductivity with temperature for two couplings; intermediate-weak ($J = 1$, Fig. 1(a)) and intermediate-strong ($J = 1.5$, Fig. 1(b)); the insets show the majority-spin densities of states. Consider first the $T = T_c$ curves (solid lines), where T_c is the ferromagnetic transition temperature [11]. The $J = 1$ curve has approximately the Drude form expected for carriers scattering off random impurities (a closer examination reveals minor differences due to density of states variations near the band edge). In the $J = 1.5$ case the density of states plot shows that an impurity band is formed and the corresponding conductivity has two structures: a low-frequency quasi-Drude peak corresponding to motion within the impurity band and a higher frequency peak corresponding to excitations from the impurity band to the main band. We observe that the frequency of the upper peak does not directly give the separation between the impurity band Fermi level and the conduction band, because the vanishing of the velocity and density of states at the band edge means that the lowest unoccupied state is not optically active.

We now turn to the temperature dependence. For the $J = 1.5$ curves we see that as T is decreased, the dc conductivity changes only very slightly, whereas the width of the low frequency peak increases and the high frequency peak moves up in energy and decreases in oscillator strength. The increase in energy of the higher frequency peak may be understood from the density of states curves, which show a weak blue-shift of the conduction band edge and a broadening of the impurity band. The counter-intuitive broadening (as T is decreased) of the lower frequency peak arises because, as the spins order, the binding of the carriers to the impurity spins

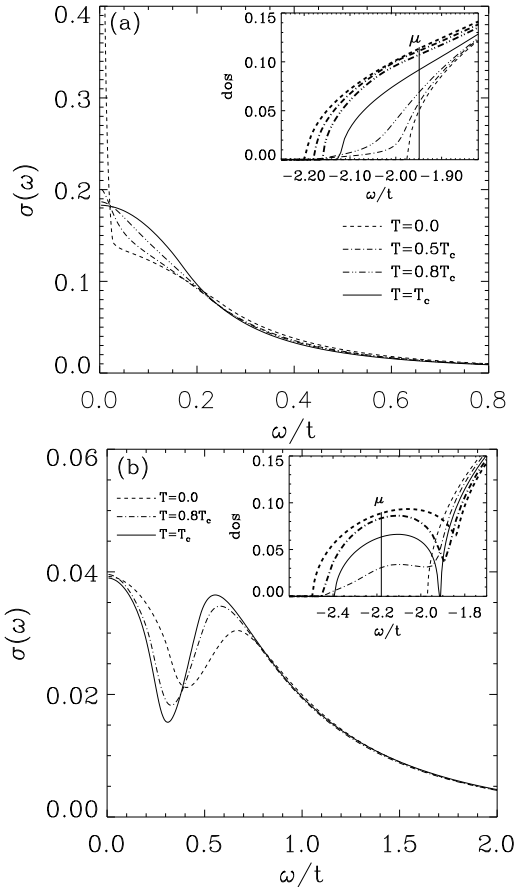


FIG. 1. Temperature dependence of optical conductivity for (a) $J = 1.0t$, $x = 0.05$, $n = 0.02$ with $T_c = 5.95 \times 10^{-3}t/k_B$, and (b) $J = 1.5t$, $x = 0.05$, $n = 0.02$ with $T_c = 1.24 \times 10^{-2}t/k_B$. Insets show the density of states for both majority spin (thick curves) and minority spins (thin curves). The vertical lines show the zero temperature chemical potentials.

increases (as seen from the increase in separation between the chemical potential and the edge of the main band) corresponding to an increase in the basic scattering rate. The weak T -dependence of the dc conductivity occurs because the increase in scattering rate is compensated by another effect. Because the impurity band is spin-polarized carriers which are bound to impurity site must have spins parallel to impurity spin. Thus, as the spins order ferromagnetically, basic ability of carriers to move in the impurity band increases. This physics is familiar from the CMR materials [14] and corresponds to an increase in conduction band oscillator strength.

Consider next the $J = 1$ curve, where two effects occur as T decreases. First, the main quasi-Lorentzian peak decreases slightly in amplitude and increases slightly in half-width. The increase in width is due to increased carrier-spin coupling as mentioned above. Second, a new narrow peak appears. As can be seen from the inset in Fig. 1(a), at $T = 0$ for this carrier concentration, the minority spin-band is slightly occupied and the sharply

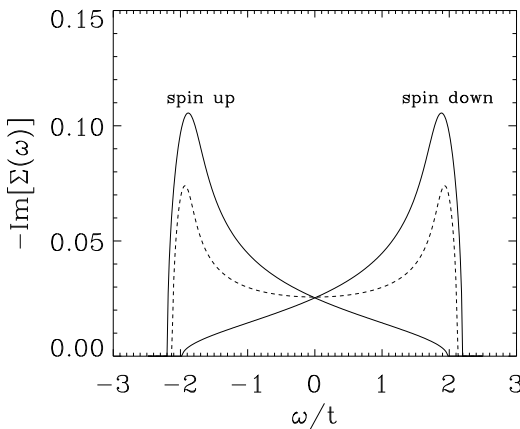


FIG. 2. Imaginary part of the self energy as a function of the frequency for $J = 1.0t$ and $x = 0.05$. Solid (dashed) curves show the self energy at $T = 0$ ($T = T_c$).

peaked conductivity occurs because this small density of carriers is very weakly scattered.

To understand the small scattering rate it is helpful to consider the Born approximation, which would lead to $\text{Im}[\Sigma] \sim xN(E_F)J^2$ with x the magnetic impurity concentration, $N(E_F)$ the density of states, and J the carrier-spin coupling. The combination of the small value of x and the small density of states at the band edge leads to a small scattering rate (in the Born approximation). Now consider corrections to the Born approximation. For the majority spin band, increase of J leads to the formation of a spin-polarized bound state, so the corrections to the Born approximation must be such as to strongly increase the effective scattering rate. On the other hand, for minority spin carriers the increase of J leads to an antibound state at the top of the band, so that at the physically relevant lower band edge, the corrections must be such as to decrease the effective scattering rate. Quantitatively, these effects are quite large. Fig. 2, for example, shows the calculated imaginary part of the $T = 0$ majority and minority spin self energy for $J = 1$.

We now consider the density dependence of the conductivity. Fig. 3(a) shows the evolution of $\sigma(\omega, T = 0)$ with carrier density for $J = 1$. At very low density ($n = 0.01$) the minority spin band is unoccupied and the behavior associated with the majority spin band is observed. A sharp peak occurs when the minority band begins to be populated. Fig. 3(b) shows the evolution of $\sigma(\omega, T = 0)$ with n for the ‘impurity-band’ case $J = 1.5$. At very small n the conductivity is dominated by the ‘impurity band’ contribution, with a relatively weak feature corresponding to transitions from the impurity band to the main band. As the carrier density is increased the band oscillator strength in transitions between the impurity and main band increases dramatically, both in absolute terms and relative to the intra-impurity band transitions. When the Fermi level crosses into the minority spin band (note that the minority spin impurity band is at the upper band edge; here we have only main-band states) an

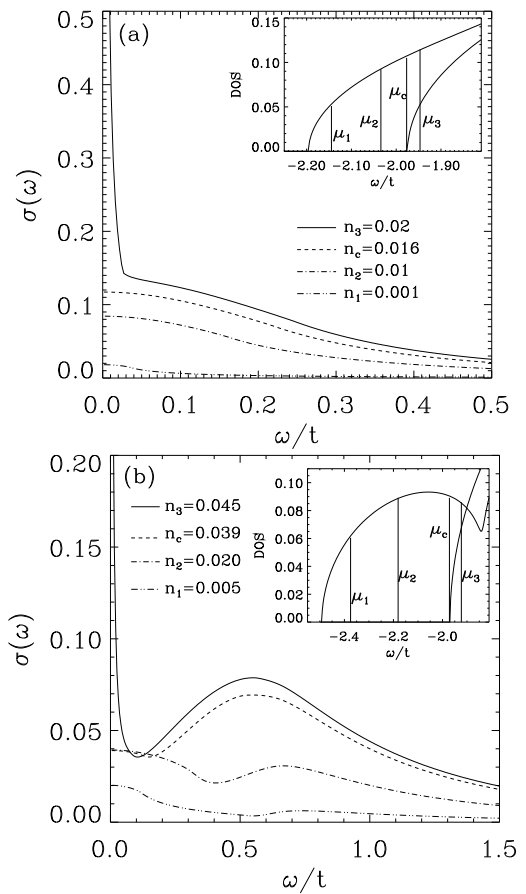


FIG. 3. Density dependence of optical conductivity for (a) $J = 1.0t$, $x = 0.05$, and (b) $J = 1.5t$, $x = 0.05$ for $T = 0K$. Inset shows the density of states and the chemical potentials at zero temperature. For $n > n_c$ the minority subband is occupied.

additional sharp low frequency component is observed.

Fig. 4 shows the sensitivity of the predicted behavior to potential scattering. The main panel shows the evolution of the conductivity as the scalar part W of the electron-impurity potential is varied. We study here a case in which at zero scalar potential the impurity band is well formed. As the potential is made more attractive, the impurity band features become more pronounced; as it is made more repulsive, the impurity band rapidly rejoins the main band and the extra feature in the conductivity is lost. The inset shows the dependence of the transition temperature on density at different potential strengths. We see that for attractive potential the dependence on potential strength is weak, but as the potential is made more repulsive the impurity band is destroyed and T_c decreases.

It is instructive to compare the optical properties of DMS to those of another system with strong carrier-spin couplings, namely CMR manganites such as $(\text{La}_{1-x}\text{Ca}_x)\text{MnO}_3$ [14]. In CMR, instead of being dilute random impurities as in DMS, the Mn ions form an ordered lattice. They possess large local moment, to which

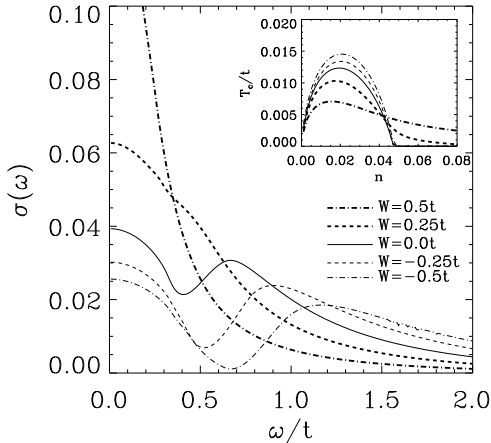


FIG. 4. Optical conductivities for various of impurity potential scattering. Inset shows the transition temperature as a function of density.

mobile carriers are very strongly coupled. Thus instead of a spin-polarized impurity band, there is a spin-polarized conduction band, sufficiently well separated from other bands in the solid that the contribution to the optical conductivity arising from it may be clearly identified and analyzed [13]. The periodic arrangement of the Mn sites means that (in the absence of other physics) the scattering rate decreases as T is lowered unlike in the DMS system. The conductivity turns out to be most usefully characterized by its integrated area (spectral weight), and the change of this quantity was shown to be a good predictor of the magnetic transition temperature [17].

These CMR ideas have limited applicability to the DMS systems. For $J < 1$ the physics is of extended states scattered by defects, and this is sufficiently different from the CMR situation that the spectral weight in DMS is not related in a useful manner to T_c in this weak coupling situation. However, as J is increased and the spin-polarized impurity band develops the physics becomes more analogous to that of CMR. For example, in Fig. 1(b) the two structures in the conductivity are relatively well separated, and the spectral weight in the lower feature increases as T decreases below T_c . For $J > 2$ (not shown) the low feature becomes completely separated from the upper one. We therefore define an effective ‘impurity band spectral weight’ for $J > 1$ by integrating the conductivity from $\omega = 0$ to the conductivity minimum. We find again that the changes in ‘impurity band spectral weight’ are very weak in DMS systems relative to those observed in CMR materials, so that spectral weight ideas useful in CMR do not carry over to DMS. This is an important qualitative distinction between DMS and CMR materials.

To summarize, we have shown that the frequency, density, and temperature dependence of the conductivity contains important information about the physics of dilute magnetic semiconductors; in particular the formation of a spin-polarized impurity band leads to a peak

centered at a non-zero frequency. We present several, at first sight, counterintuitive findings. We find an *increase* in scattering rate as T is decreased, signalling enhanced carrier-spin coupling with increasing spin alignment. We also show that in certain doping and coupling regimes a very narrow conductivity peak could occur corresponding to a slightly occupied minority spin band. It occurs because the repulsive interaction between local moments and ‘wrong-spin’ carriers suppresses the carrier amplitude at the impurity site, reducing the effective carrier-spin coupling and consequently narrowing the wrong-spin conductivity peak; in addition in three dimensions the vanishing of the density of states at the band edge further decreases the rate. This suggests that a small occupation of the minority band could be quite dangerous from the spintronic applications point of view, particularly in three dimensional devices.

Finally, we note that the most interesting phenomena involve intermediate couplings, intermediate temperatures and non-zero frequency response. This regime is very difficult to treat by standard analytical or numerical methods; it is therefore fortunate that the dynamical mean field method allows access to this regime.

We thank H. D. Drew and A. Chattopadhyay for helpful conversations and DARPA(E.H.H. and S.D.S.), US-ONR (E.H.H and S.D.S.), and the University of Maryland/Rutgers NSF-DMR-MRSEC (A.J.M.) for support.

-
- [1] H. Ohno, Science **281**, 951(1998); J. Magn. Magn. Mater. **200**, 110(1999).
 - [2] H. Ohno *et al.*, Appl. Phys. Lett. **69**, 363 (1996); A. Van Esch *et al.*, Phys. Rev. B **56**, 13103(1997).
 - [3] F. Matsukura *et al.*, Phys. Rev. B **57**, R2037(1998).
 - [4] M. Reed *et al.*, Appl. Phys. Lett. **79**, 3473 (2001); N. Theodoropoulou *et al.*, cond-mat/0201492 (2002).
 - [5] H. Akai, Phys. Rev. Lett **81**, 3002(1998).
 - [6] T. Dietl *et al.*, Science **287**, 1019(2000).
 - [7] V. I. Litvinov and V. K. Dugaev, Phys. Rev. Lett. **86**, 5593(2001).
 - [8] T. Dietl, cond-mat/0201282; J. König *et al.*, cond-mat/0111314.
 - [9] M. Berciu and R. N. Bhatt, Phys. Rev. Lett. **87**, 7203 (2000).
 - [10] A. Kaminski and S. Das Sarma, cond-mat/0201229 (2002); C. Timm *et al.*, cond-mat/0201411 (2002).
 - [11] A. Chattopadhyay *et al.*, Phys. Rev. Lett. **87**, 227202-1 (2001).
 - [12] S. Das Sarma, Am. Scientist **89**, 516 (2001).
 - [13] M. Quijada *et al.*, Phys. Rev. B **58**, 16093 (1998).
 - [14] See e.g. *Colossal Magnetoresistive Oxides*, Y. Tokura, ed. (Gordon and Breach, 1999).
 - [15] A. Georges *et al.*, Rev. Mod. Phys **68**, 13 (1996).
 - [16] S. Sanvito, *et al.*, Phys. Rev. B **63**, 165206(2001).
 - [17] A. Chattopadhyay *et al.*, Phys. Rev. B **61**, 10738 (2000).